11th World Congress on Computational Mechanics (WCCM XI)
5th European Conference on Computational Mechanics (ECCM V)
6th European Conference on Computational Fluid Dynamics (ECFD VI)
E. Oñate, J. Oliver and A. Huerta (Eds)

A 16-NODE HYBRID-TREFFTZ PERFORATED ELEMENT FEATURING 8 NODES ON THE HOLE BOUNDARY

C. HENNUYER[*,†], N. LECONTE[†], B. LANGRAND[*] AND E. MARKIEWICZ[†]

[*] Onera – The French Aerospace Lab, F-59045 Lille, France
e-mail: claire.hennuyer@onera.fr

[†] LAMIH UMR CNRS 8201, University of Valenciennes, F-59313 Valenciennes, France

Key words: Hybrid-Trefftz, Super-Element, Riveted joint modelling, Structural computations

Abstract. The Finite Element (FE) computations of complete aircraft structures subjected to impact loads requires the use of "super-elements" for the modelling of the riveted assemblies. Macro-elements for the fastener have been developed and validated, but, the structural embrittlement caused by holes in the sheets is not taken into account in this modelling. Some of the authors of the paper formulated and validated a hybrid-Trefftz perforated super-element able to take into account the stress concentrations due to the hole. The hole boundary however was intrinsically a load-free analytical boundary making impossible the interaction of the super-element for the perforated plate with the rivet macro-models. In this paper, a new 16-node hybrid-Trefftz perforated super-element featuring 8 nodes on the hole boundary is formulated in order to model this interaction thanks to the new nodes and the FE hole boundary. The new perforated super-element is first validated by considering no loads applied on the nodes of the hole boundary. It is shown that the results obtained with the new super-element are very accurate whatever the test-case considered (e.g., tension, shear) and that the super-element is cost-efficient. The second step of the validation, which consists in considering, in the test-cases, nodal concentrated forces applied on the hole boundary, is in progress.

1 Introduction

Finite element analysis of airframe under High Velocity Impacts hardly succeeds in representing the failure of the structure when it occurs in riveted joint areas. However, experimentations show that the aircraft structure survivability is tightly related to the mechanical behaviour of riveted assemblies. The loads that occur in the riveted area can result in fasteners rupture and in cracks initiation along the hole boundaries in the sheets, which can lead to the catastrophic loss of the aircraft (cracks propagation along rivet lines, dismantlement of structural parts). Consequently, in order to properly predict the structure survivability, it is necessary to model accurately the behaviour of riveted assemblies in structural computations. Because of the large difference in scale between the aircraft and the assembly, and the large number of fasteners on complete structures, a refined FE modelling of each assembly is obviously not suitable to take into account the influence of the assemblies within the FE computation. For several years, the research in this domain is focused on the development of "macro-elements". The assembly is often represented with 1D element whose nodes are connected to two conventional shell elements using kinematic conditions.

At first, macro-elements (1D beam, spring) dedicated to the modelling of fasteners have been formulated and validated. The most advanced formulations are able to describe the non-linear behaviour of the rivet until rupture [1, 2]. However, the experimental and computational results comparison has shown that the structural stiffness was overestimated by the numerical model and the plastic strain within the FE shell elements connected to rivets was not efficiently enough predicted so as to initiate the failure of the sheet metal plates [3, 4]. The assembly modelling suffers in fact from a lack of representativeness. The structural embrittlement caused by holes in the sheets is not introduced in the conventional shell elements to which rivets macro-elements are connected. The forces are moreover not correctly transferred from the rivet macro-element to the shell elements. The interaction between the fastener and the perforated sheets is improperly taken into account, and, several failure modes (e.g., bearing, pull-through) can not be handled.

In order to improve the modelling of riveted assemblies in structural computations, "super-elements" featuring a hole have been studied. Piltner [5], Zhang *et al.* [6], Dhanasekar *et al.* [7], and Qin *et al.* [8] developed perforated super-elements for various applications (computation of stress concentration factor, mechanical analysis of heterogeneous material, etc.). More recently, Leconte *et al.* [9] developed a 8-node perforated super-element for the modelling of riveted assemblies (plane stress/strain element). It allows to compute accurately and efficiently (cost-efficient due to few degrees of freedom (dofs)) the displacement and stress fields in particular around the hole for any external load case considered in plane elasticity. Nevertheless, even if the stress concentrations due to the hole in the sheet can now be taken into account in structural computations, the interaction between both the rivet and the sheet macro-models can not be handled because the hole boundary of the perforated super-element is a load-free analytical boundary, preventing any connections with rivet elements.

The authors propose to formulate a new perforated super-element which features nodes on the hole boundary in order to allow the interaction with a rivet macro-element *via* these new nodes and the FE hole boundary. The proposed formulation is based on the previous 8-node super-element to which 8 new additional nodes have been added on the hole boundary. The number of nodes placed on the hole boundary of the new super-element is chosen by the authors so that the super-element is efficient (compromise between the accuracy and the number of dofs) and that the interaction between the proposed super-element and the rivet macro-element is properly modelled. The developments and the validation of a 16-node Hybrid-Trefftz (HT) perforated super-element featuring 8 nodes for the hole boundary which can be loaded is consequently presented in this paper.

2 Formulation of a new perforated super-element featuring nodes on the hole boundary

The new perforated super-element (Fig. 1) is a generalization of the previous 8-node hybrid-Trefftz FE developed by Leconte *et al.* [9], which did not feature internal nodes on the hole. Its formulation is based on a HT displacement variational principle in which the hole boundary, denoted by S_p, is now taken into account. The super-element is supposed to be completely surrounded by conventional FEs, and, is formulated so that the displacement compatibility is required and ensured on the external inter-element boundary only, denoted by S_i. The displacement compatibility is however not ensured on the internal boundary, because the case of an inclusion would be considered otherwise [10]. The vector of assumed boundary displacements along the external boundary $\widetilde{\mathbf{u}}$ is thus introduced in the formulation such as $\widetilde{\mathbf{u}} = \widetilde{\mathbf{N}}\widetilde{\mathbf{q}}_{ext}$, with $\widetilde{\mathbf{q}}_{ext}$ the external nodal displacements and $\widetilde{\mathbf{N}}$ the shape functions matrix computed according to the conventional adjacent FEs. The homogeneous solutions $\mathbf{u}^h$ and $\mathbf{T}^h$ (traction vector) are expressed by $\mathbf{u}^h = \mathbf{Nc}$ and $\mathbf{T}^h = \mathbf{Pc}$ where $\mathbf{c}$ is a vector of parameters known as generalized dofs, $\mathbf{N}$ and $\mathbf{P}$ are the interpolation functions computed from complex variable method [11].

The accuracy of the interpolation functions of the 16-node super-element (with internal nodes) has been first studied. The increase in the parameters number of the solution (which is related to the nodes number) has shown a little influence on the accuracy of the obtained mechanical fields. The differences come from the introduction of additional spurious parameters *via* new series terms. The mechanical fields within the super-element are whatever properly predicted by the interpolation functions and especially close to the hole [12].

The formalism proposed by Soh [13, 14] has been considered to express the displacement and stress fields depending on physical dofs, $\mathbf{d}$, instead of the previous generalized ones $\mathbf{c}$ (Eq. (1)). It is indeed necessary to distinguish the dofs located on both the external and internal boundaries, and also to place 8 nodes on particular locations on the hole boundary.

$$\mathbf{u}^h = \mathbf{Ud} \text{ and } \mathbf{T}^h = \mathbf{Md} \tag{1}$$

where $\mathbf{d}$ is the vector of external <u>and</u> internal nodal displacements, and, $\mathbf{U}$ and $\mathbf{M}$ are the shape functions of the super-element.

Loads applied on the hole boundary are finally taken into account in the element formulation by a particular solution, $(\mathbf{u}^p, \mathbf{T}^p)$, which is added to the previous homogeneous one. The particular solution considered here is related to concentrated forces applied on the nodes of the hole boundary [15]. The interaction with the rivet model can then be established.

The minimization of the obtained functional Π_{HT} (Eq. (2)) with respect to $\mathbf{d}$ and $\widetilde{\mathbf{q}}_{ext}$, respectively, leads to a system where the internal dofs are eliminated from the formulation. Nodes placed on the hole boundary can not consequently be loaded, which is contrary to what we look for.

$$\Pi_{\mathrm{HT}}\left[\mathbf{d}, \widetilde{\mathbf{q}}_{ext}\right] = \frac{1}{2}\mathbf{d}^t\mathbf{H}\mathbf{d} + \mathbf{d}^t\mathbf{L}\widetilde{\mathbf{q}}_{ext} + \mathbf{d}^t\mathbf{r}^c + \widetilde{\mathbf{q}}_{ext}^t\mathbf{r}^d \tag{2}$$

with $\mathbf{H} = \int_{S_p} \mathbf{M}^t\mathbf{U}\ dS - \int_{S_i} \mathbf{M}^t\mathbf{U}\ dS$, $\mathbf{L} = \int_{S_i} \mathbf{M}^t\widetilde{\mathbf{N}}\ dS$, $\mathbf{r}^d = \int_{S_i} \widetilde{\mathbf{N}}^t\mathbf{T}^p\ dS$, and

$$\mathbf{r}^c = \frac{1}{2}\left[\int_{S_p} \mathbf{M}^t\mathbf{u}^p\ dS + \int_{S_p} \mathbf{U}^t\mathbf{T}^p\ dS - \int_{S_i} \mathbf{M}^t\mathbf{u}^p\ dS - \int_{S_i} \mathbf{U}^t\mathbf{T}^p\ dS\right].$$

In order to keep $\mathbf{q}_{int}$ within the element formulation, it is first necessary to separate $\mathbf{d}$ such as $\mathbf{d} = [\mathbf{q}_{ext}^t, \mathbf{q}_{int}^t]$ in order to express Π_{HT} as a function of the overall dofs: $\mathbf{q}_{ext}$, $\mathbf{q}_{int}$ and $\widetilde{\mathbf{q}}_{ext}$. By taking the first stationary condition with respect to $\mathbf{q}_{ext}$, a linear relation between $\mathbf{q}_{ext}$ and the two others dofs vectors, $\widetilde{\mathbf{q}}_{ext}$ and $\mathbf{q}_{int}$, is thus established. The expression of $\mathbf{q}_{ext}$ is then introduced within the variational principle, so that Π_{HT} depends only on the variable $\mathbf{q} = [\widetilde{\mathbf{q}}_{ext}^t, \mathbf{q}_{int}^t]$. The expected system $\mathbf{Kq} = \mathbf{f}$ is finally obtained by taking the second stationary condition with respect to the dofs vector $\mathbf{q}$ and is presented in Eq. (3).

$$\begin{bmatrix} \mathbf{K}_{11} & \mathbf{K}_{12} \\ \mathbf{K}_{21} & \mathbf{K}_{22} \end{bmatrix} \begin{bmatrix} \widetilde{\mathbf{q}}_{ext} \\ \mathbf{q}_{int} \end{bmatrix} = \begin{bmatrix} \mathbf{f}_{ext} \\ \mathbf{f}_{int} \end{bmatrix} \tag{3}$$

The stiffness matrix $\mathbf{K}$ of the new FE is a 2×2 blocks matrix which is symmetric by construction. The two diagonal blocks of the matrix $\mathbf{K}$ represent the stiffness related to external and internal dofs respectively; the two off-diagonal blocks represent the stiffness related to the interaction between the nodes of each boundary. These are full matrices which means that there is a coupling between nodes of the hole boundary and the ones of the external boundary of the super-element. The load vector $\mathbf{f}$ is defined as a function of the vectors $\mathbf{r}^c$ and $\mathbf{r}^d$. As the latest depends on the particular solution $\mathbf{u}^p, \mathbf{T}^p$, it can be concluded that the load vector $\mathbf{f}$ corresponds effectively to the hole boundary loading. When the hole boundary is load-free, i.e. when the particular solution is supposed to be zero ($\mathbf{u}^p = \mathbf{T}^p = 0$), it can be easily observed that the load vector $\mathbf{f}$ equals to zero, which was already the case for the previous 8-node super-element. Moreover, if the new nodes are eliminated from the above developments, the formulation of the previous 8-node super-element is recovered.

3 Evaluation of the new perforated super-element

The new perforated super-element is implemented into the implicit FE code ZéBuLoN (Mines ParisTech/ONERA/NorthWest Numerics) [16, 17], and it is based on a 8-node

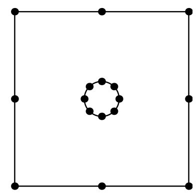

Figure 1: A 16-node HT super-element featuring 8 nodes for the hole boundary.

quadratic quadrilateral element where 8 internal nodes and an internal piecewise quadratic boundary (FE hole boundary) have been added. The inter-element boundary displacements $\widetilde{\mathbf{u}}$ are piecewise quadratic. The computation of the stiffness matrix $\mathbf{K}$ and the load vector $\mathbf{f}$ of the new super-element requires integration of vectors $\mathbf{u}$ and $\mathbf{T}$ along both the external and internal boundaries, so Gauss quadrature and 16 Gauss points per side (points and weights were taken from [18]) are used. The validation of the proposed developments is performed in two steps: (1) test-cases where no force is applied on the hole boundary are considered to check the results non-regression compared to the previous 8-node super-element; (2) test-cases where forces are applied on the hole boundary are considered to completely validate the new super-element. In this paper, only the first step of validation is presented. The second validation step is currently being addressed.

A perforated plate (size: 14 mm $\times$ 14 mm) featuring a load-free centred circular hole of radius $a = 0.2$ mm subjected to several external loads (i.e., uniaxial tension, biaxial tension, pure shear, simple shear) is considered. The material properties are $E = 74{,}000$ MPa and $\nu = 0.3$, for the Young's modulus and the Poisson's ratio respectively. Reference data are obtained thanks to a standard FE model, particularly refined close to the hole, featuring 12,000 standard quadratic 8-node elements. The implementation of the super-element is validated using a coarse mesh made of 48 standard quadratic 8-node elements and a central perforated super-element only.

The results are presented in terms of von Mises stress distribution. Results obtained with the new perforated super-element are compared, for each test-case investigated, with those provided by the reference refined FE model and the previous 8-node super-element in Fig. 2. The von Mises stress field is consistent with the studied test-case, and this for all test-cases. The same analysis can be made for each component of the stress tensor and the displacement vector, although these results are not presented here for the sake of conciseness. The results are also compared along the y-axis in Fig. 3. The distribution of displacement and stress is accurately computed and is in close agreement with the reference data, particularly close to the perforation. Besides, for an uniaxial tensile test-case, the hoop stress is slightly better evaluated with the new perforated super-element: $K_t = 2.972$, while $K_t = 2.967$ with the previous super-element (with 16 Gauss points per side too). However, for shear loads, the von Mises stress is slightly underestimated by the new 16-node super-element compared to the reference refined FE model and the previous 8-node super-element. This difference could be explained by the fact that the interpolation functions of the 16-node super-element are less accurate than the ones of the 8-node super-element, as it has been highlighted by the authors in particular for shear load cases [12]. The new super-element remains very efficient because about $0.35\,s$ (CPU) only are necessary to compute one test-case using the super-element, while $50\,s$ are necessary to compute the same problem (with the same accuracy) using the reference FE model. The computational costs increase slightly for the new super-element when compared to the previous perforated super-element ($0.3\,s$) because additional integration computations on the hole boundary are performed. It remains really cost-efficient and the costs are of the same order of magnitude that of the previous formulation.

4 Conclusions

A new perforated super-element featuring nodes on the hole boundary is formulated in order to improve the modelling of riveted assemblies in structural computations. The proposed super-element allows, on the one hand, to take into account the stress concentrations due to the hole in the sheet requiring only few dofs; and, on the other hand, to establish the interaction between the rivet macro-element and the perforated super-element thanks to the new nodes located on the hole boundary. Interaction forces can be applied to these new nodes, implying displacements and stresses within the super-element.

Only the first step of the validation of the new perforated super-element has been presented. Forces applied to the hole nodes are omitted for this first validation step. The capability of the new super-element to predict the distribution of the displacement and stress fields around the hole boundary and within the element under several external loads is tested. The results obtained for uniaxial or biaxial tension and simple or pure shear have shown that the new perforated super-element is very accurate and efficient. The second step of the validation, which consists in applying concentrated forces on the nodes of the hole boundary, is currently being handled.

Once the new super-element with internal nodes fully validated for elastic material behaviour, its extension to non-linear material behaviours will be studied and addressed. Future works will concern the extension to a shell formulation, suitable for structural aircraft computations.

Acknowledgements

The present research work has been supported by Onera, the International Campus on Safety and Intermodality in Transportation, the Nord-Pas-de-Calais Region, the European Community, the Regional Delegation for Research and Technology, the Ministry of Higher Education and Research, and the National Center for Scientific Research. The authors gratefully acknowledge the support of these institutions.

REFERENCES

[1] Combescure, A., Delcroix, F., Caplain, L., Espanol, S. and Eliot, P. A finite element to simulate the failure of weld points on impact. *Int. J. Impact Eng.* (2003) **28**:783–802.

[2] Langrand, B., Deletombe, E., Markiewicz, E. and Drazétic, P. Riveted joint modelling for numerical analysis of airframe crashworthiness. *Finite Elem. Anal. Des.* (2001) **38**:21–44.

[3] Langrand, B., Patronelli, L., Deletombe, E., Markiewicz, E. and Draztic, P. An alternative numerical approach for full scale characterisation for riveted joint design. *Aerospace Science and Technology* (2002) **6**:343–354.

[4] Langrand, B., Bayart, A.S., Chauveau, Y. and Deletombe, E. Assessment of multi-physics FE methods for bird impact modelling - Application to a metallic riveted airframe. *Int. J. Crashworthiness* (2002) **7**:415–428.

[5] Piltner, R. Special finite elements with holes and internal cracks. *Int. J. Num. Meth. Engng.* (1985) **21**:1471–1485.

[6] Zhang, J. and Katsube, N. A polygonal element approach to random heterogeneous media with rigid ellipses or elliptical voids. *Comput. Method. Appl. M.* (1997) **148**:225–234.

[7] Dhanasekar, M., Han, J. and Qin, Q.H. A hybrid-Trefftz element containing an elliptic hole. *Finite Elem. Anal. Des.* (2006) **42**:1314–1323.

[8] Qin, Q.H. and He, X.Q. Special elliptic hole elements of Trefftz FEM in stress concentration analysis. *Journal of Mechanics and Mems* (2009) **1**:335–348.

[9] Leconte, N., Langrand, B. and Markiewicz, E. On some features of a plate hybrid-Trefftz displacement element containing a hole. *Finite Elem. Anal. Des.* (2010) **46**:819–828.

[10] Cesari, F., Furgiuele, F.M. and Martini, D. Analisi di strutture piane in materiale eterogeneo con l'elemento finito ibrido. *XXX AIAS* Alghero (Italy) (2001) 1093–1101.

[11] Muskhelishvili, N.I. *Some Basic Problems of the Mathematical Theory of Elasticity.* Noordhoff, Groningen, Holland, (1953).

[12] Hennuyer, C., Leconte, N., Langrand, B. and Markiewicz, E. Toward the modelling of riveted assemblies by super-elements in fast dynamics. *Mechanics & Industry* (2014) *In Press.*

[13] Soh, A.K. and Long, Z.F. A high precision element with a central circular hole. *Int. J. Solids Struct.* (1999) **36**:5485–5497.

[14] Yang, C.H. and Soh, A.K. Modeling of voids/cracks and their interactions. *Theor. Appl. Fract. Mec.* (2002) **38**:81–101.

[15] Sih, G.C. Stress distribution around an ovaloid hole under arbitrary concentrated forces. *Appl. Sci. Res.* (1964) **12A**:378–390.

[16] Feyel, F. Some new techniques regarding the parallelisation of ZéBuLoN, an object oriented finite element code for structural mechanics. *Math. Model. Numer. Anal.* (2002) **36**:923–936.

[17] Z-SET/ZéBuLoN. Non-linear finite element solver of the Z-SET suite. (2011) `http://www.zset-software.com/`

[18] Abramowitz, M. and Stegun, I.A. *Handbook of Mathematical Functions with Formulas, Graphs, and Mathematical Tables.* Dover Publications, New York, (1970).

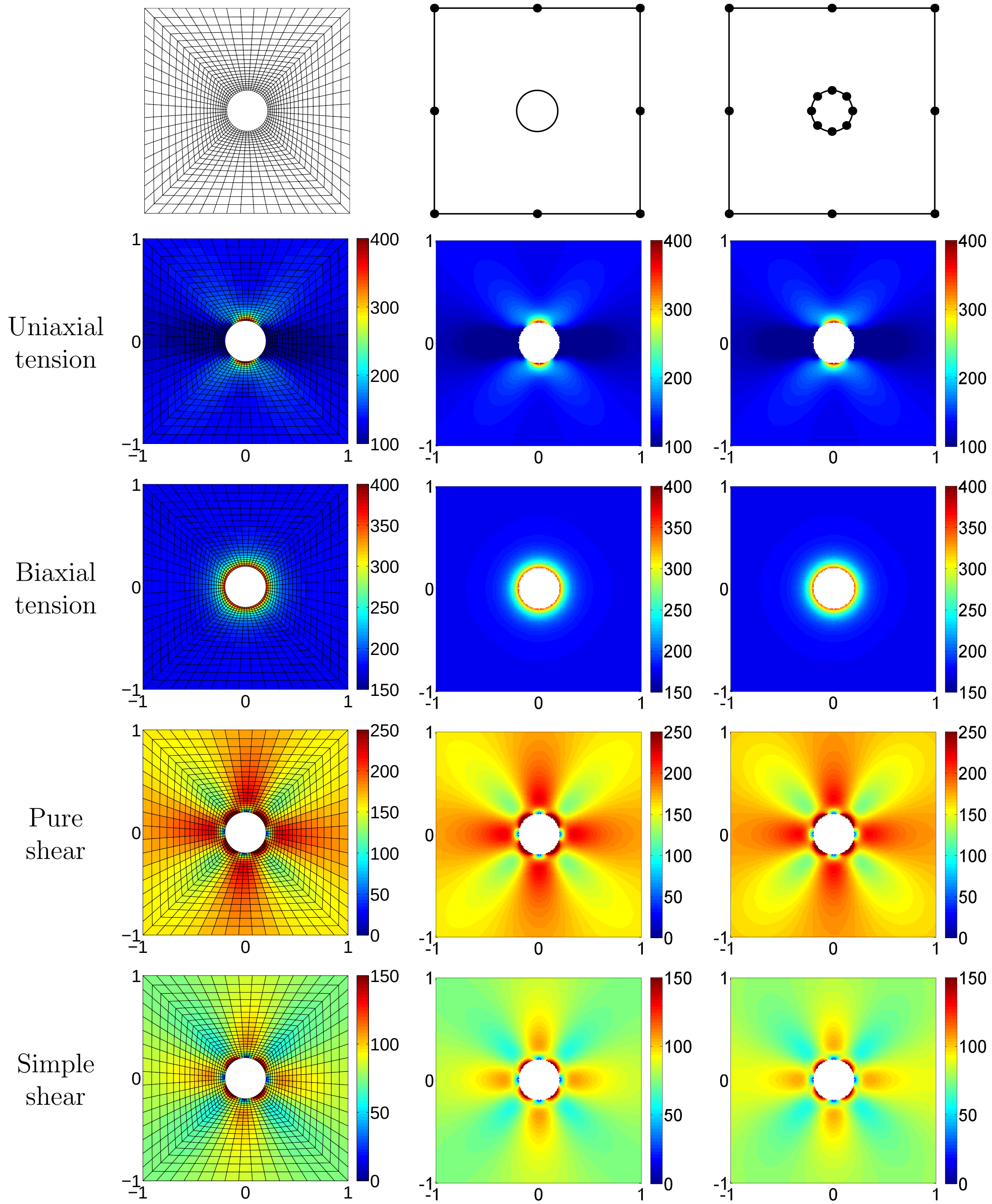

Figure 2: Comparison of the von Mises stress distribution between the standard FEM (left), the 8-node super-element (center), and the new 16-node super-element (right).

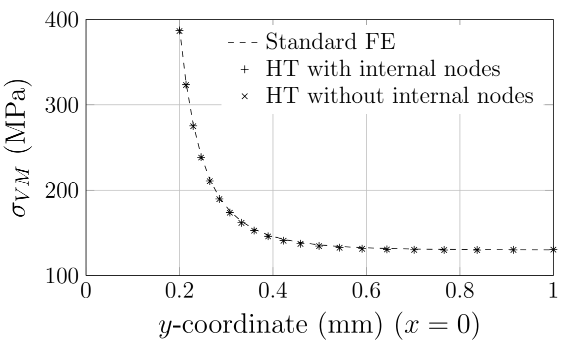

(a)

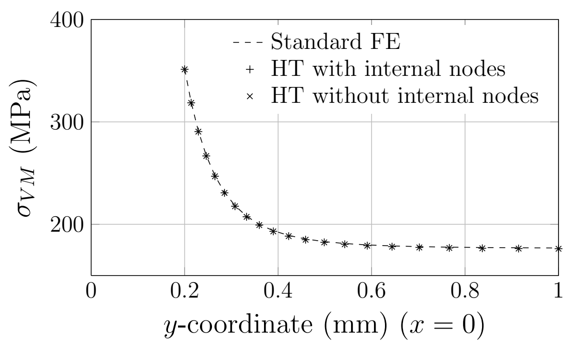

(b)

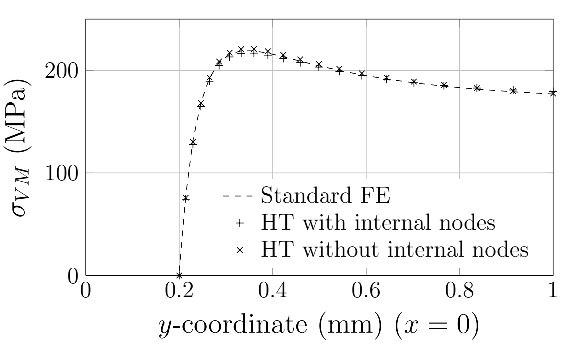

(c)

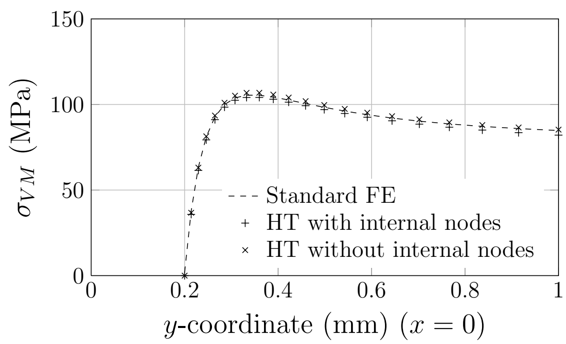

(d)

Figure 3: Comparison of the von Mises stress distribution along the y-axis between the standard FE analysis, the 8-node super-element (without internal nodes), and the new 16-node super-element (with internal nodes) (a) Uniaxial tension (b) Biaxial tension (c) Pure shear (d) Simple shear.